

S.M. Dubiel · B. Zablotna-Rypien · J.B. Mackey  
J.M. Williams

## Magnetic properties of human liver and brain ferritin

Received: 10 July 1998 / Revised version: 29 September 1998 / Accepted: 9 October 1998

**Abstract** Human brain (*globus pallidus*) and liver tissues were investigated by means of electron microscopy (EM), Mössbauer spectroscopy (MS) and SQUID magnetometry techniques. Based on MS measurements, the iron present was identified to be in the ferritin-like form (61–88%) and in the form of a low-spin iron species (the balance). Its overall concentration was estimated as 1.5(3) mg in the brain and 2.4(5) mg in the liver, per gram of lyophilized tissue. The average core diameter was determined by EM measurements to be equal to 7.5(1.3) nm for the liver and 3.3(5) nm for the brain. Magnetization measurements carried out between 5 and 300 K yielded an estimation of an average blocking temperature,  $\langle T_B \rangle$ , as equal to 6.7 K and 8.5 K for the liver and the brain, respectively. From the dependence of  $\langle T_B \rangle$  on the external magnetic field it was concluded that the ferritin-like cores in the studied samples can be regarded as non-interacting particles. Finally, the uniaxial magnetic anisotropy constant was determined to be  $6 \times 10^3$  J/m<sup>3</sup> for the liver and  $4 \times 10^4$  J/m<sup>3</sup> for the brain.

**Key words** Human liver · Human brain · Ferritin · Electron microscopy · Mössbauer spectroscopy

### Introduction

Iron is the most abundant transition metal element in living organisms, and it plays a crucial role in many vital metabolic functions such as oxygen transport and electron transfer. The positive role it was believed to play in human health has been recently questioned. Unbound iron is

highly toxic, acting as a catalyst for the production of free radicals which can ultimately lead to cellular damage. Several human diseases, including neurodegenerative Parkinson and Alzheimer diseases, have recently been postulated to be related to the role of iron (Lauffer 1992).

Nature has, however, developed an iron-storage molecule which acts as an internal iron reserve, storing the iron in a physiologically safe non-toxic form known as ferritin. Ferritin-like proteins have been found in many diverse organisms, ranging from primitive bacteria cells to higher organisms including *Homo sapiens*. In the latter, ferritin can be found in various organs such as liver, spleen, heart and brain, and also in the blood, and its enhanced level is usually indicative of a disease (Bauminger and Nowik 1998).

Investigation of ferritin is also of interest to the physicist, because ferritin cores, which can accommodate up to 4500 Fe(III) atoms, exhibit superparamagnetic properties characteristic of magnetic nanoparticles.

In this Letter, magnetic properties of ferritin-like particles found in a human liver and brain (*globus pallidus*) are described and discussed.

### Materials and methods

Samples to be investigated were taken from the brain (*globus pallidus*) and liver at autopsy using plastic blades. One brain sample, hereafter referred to as fresh, was sealed in a lucite container of 1 ml volume and 1.5 cm<sup>2</sup> cross section and frozen in dry ice immediately after autopsy. Another brain sample and one liver sample were lyophilized and stored at room temperature.

Three experimental techniques, Mössbauer spectroscopy (MS), electron microscopy (EM) and SQUID magnetometry, were applied in the investigation of the samples. MS was used to identify what iron species were present and to estimate their concentration, EM to determine the size distribution of the ferritin cores, and SQUID magnetometry to measure magnetic properties of the samples.

S.M. Dubiel (✉) · B. Zablotna-Rypien  
Faculty of Physics and Nuclear Techniques,  
The University of Mining and Metallurgy (AGH),  
al. Mickiewicza 30, PL-30-059 Kraków, Poland  
e-mail: dubiel@novell.ftj.agh.edu.pl

J.B. Mackey · J.M. Williams  
Physics Department, University of Sheffield,  
Sheffield S3 7RH, UK

Mössbauer spectra were recorded in a transmission geometry by means of a standard spectrometer on samples whose mass was  $\approx 200$  mg. A 40 mCi source of  $^{57}\text{Co}/\text{Rh}$  kept at room temperature was used to supply the 14.4 keV gamma rays, which were detected by a proportional counter. During measurements the samples were kept in a gas-flow cryostat, and their temperature  $T$  was varied between 80 K and 290 K with an accuracy of 0.1 K. A least-squares fit to the Mössbauer data yields values for the hyperfine parameters (the isomer shift, IS, the quadrupole splitting, QS) as well as the line width,  $\Gamma$ , and the line intensities.

TEM micrographs were taken on ferritin particles isolated from the tissue by means of a JEM 1200 ExII electron microscope operating at 80 keV. Particle size determinations were made by measurement of 60 protein iron-cores.

Magnetization measurements were carried out on the lyophilized samples (of mass  $\approx 100$  mg) using the MPMS-5 SQUID magnetometer from Quantum Design. It has a temperature range of 5–300 K and can produce magnetic fields up to 5 T. The zero-field-cooled magnetization curve,  $M_{\text{ZFC}}$  versus  $T$ , was measured on the samples that were initially cooled to 5 K in zero field. Then a constant field was applied and the magnetization measured in that field as a function of increasing temperature. The field-cooled magnetization curve,  $M_{\text{FC}}$  versus  $T$ , was then recorded on cooling the sample down to 5 K in the field. The fields applied in the present study were between 50 G and 4000 G for the liver and 50 G and 1400 G for the brain.

## Results and discussion

### Mössbauer effect

Figure 1 shows a  $^{57}\text{Fe}$  Mössbauer spectrum recorded at 80 K on a sample of horse spleen ferritin from Sigma, which was used as a standard. It was fitted in terms of a doublet whose best-fit spectral parameters are as follows: IS =  $0.45(1)$  mm/s (relative to that of  $\alpha\text{-Fe}$ ), QS =  $0.70(1)$  mm/s and  $\Gamma = 0.62$  mm/s. Mössbauer spectra of the investigated samples are presented in Fig. 2. In comparison with that shown in Fig. 1 they have an additional subspectrum, so they were therefore successfully fitted in terms of two doublets. The best-fit spectral parameters thus obtained are displayed in Table 1. They prove that the investigated samples contain iron in the form of ferritin (61–88%) and a low-spin iron (balance) (St. Pierre et al. 1992). The content of the latter seems to be enhanced by the lyophilization.

Knowing the concentration of the iron in the standard sample,  $C_0$ , its content in the investigated samples,  $C_x$ , was determined from the formula

$$C_x = C_0(S_x/S_0) \quad (1)$$

where  $S$  stands for the normalized spectral area. The values obtained can be seen in Table 1 and agree well with

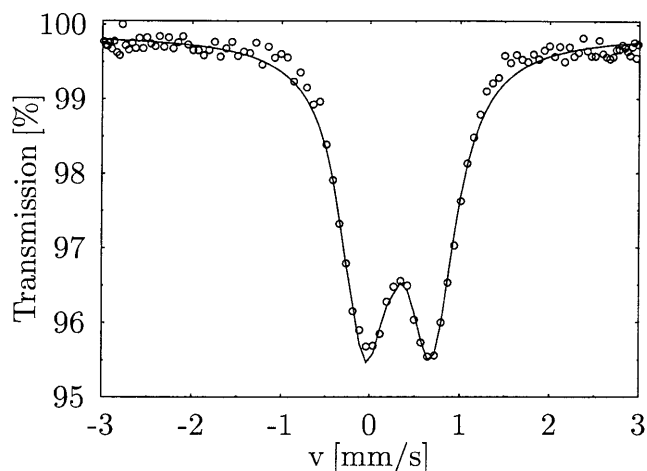


Fig. 1  $^{57}\text{Fe}$  Mössbauer spectrum of a horse spleen ferritin from Sigma recorded at 80 K

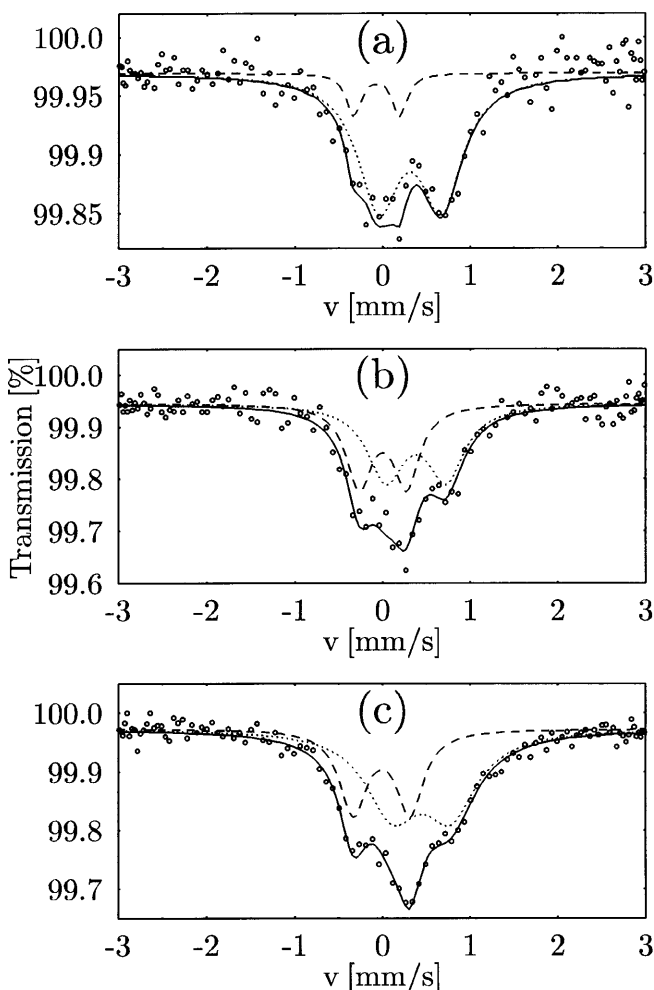


Fig. 2a–c  $^{57}\text{Fe}$  Mössbauer spectra recorded at 80 K for **a** fresh and **b** lyophilized sample of brain (*globus pallidus*) and **c** lyophilized sample of liver

**Table 1** The best-fit spectral parameters obtained for fresh (fr) and lyophilized (ly) samples. IS stands for the isomer shift (relative to

that of  $\alpha$ -Fe), QS is for the quadrupole splitting,  $\Gamma$  for the line width at half maximum,  $A$  for the abundance (%) and  $C_x$  for the iron con-

Sample	IS <sub>1</sub>	QS <sub>1</sub>	$\Gamma_1$	A <sub>1</sub> (%)	IS <sub>2</sub>	QS <sub>2</sub>	$\Gamma_2$	A <sub>2</sub> (%)	C <sub>x</sub>
Brain (fr)	0.44 (12)	0.76 (15)	0.54 (3)	88 (7)	0.05 (5)	0.62 (6)	0.22 (3)	12 (3)	0.39 (13)
Brain (ly)	0.51 (5)	0.70 (4)	0.54 (4)	61 (8)	0.10 (1)	0.54 (3)	0.32 (3)	39 (7)	1.5 (3)
Liver (ly)	0.58 (9)	0.66 (1)	0.76 (5)	66 (7)	0.12 (1)	0.64 (4)	0.38 (4)	34 (7)	2.4 (5)

those available in the literature (Galazka-Friedman and Friedman 1997).

### Electron microscopy

The size distribution of ferritin cores isolated from the liver tissue is presented in Fig. 3. The average core diameter is equal to 7.5(1.3) nm, which agrees with estimates found for ferritin from human spleen, heart and liver (St. Pierre et al. 1992). However, similar measurements done on the brain-ferritin cores yielded for the average diameter the value of 3.3(5) nm (J. Galazka-Friedman, personal communication, 1997). This means that the volume of the liver-ferritin cores is one order of magnitude larger than that of the brain-ferritin.

### SQUID magnetometry

Examples of typical field-cooled (FC) and zero-field-cooled (ZFC) magnetization curves obtained are shown in Fig. 4. Their characteristic features are: (1) a maximum in the  $M_{ZFC}$  curve, whose position is usually associated with the average blocking temperature,  $\langle T_B \rangle$  (examples of the maxima recorded for the brain can be seen in Fig. 5) and (2) a bifurcation of the two curves at  $T_B$  which defines a point of an irreversibility line between reversible and irreversible behaviour.  $T_B$  corresponds to the blocking temperature of the largest particle volume (Mohie-Eldin et al. 1994). It is of interest to study the influence of  $B$  both on  $\langle T_B \rangle$  and on  $T_B$ . According to Luo et al. (1991) and Hanson et al. (1995), an increase of  $\langle T_B \rangle$  with  $B$  indicates the particles do not interact with each other. If  $B$  causes a decrease of  $\langle T_B \rangle$ , there is an interaction between the particles.

The data shown in Fig. 6 give evidence, both for the liver (open symbols) and for the brain (full symbols), that  $\langle T_B \rangle$  increases with  $B$ . This agrees with the expectation that ferritin cores do not interact (they are encapsulated in a protein shell). Further evidence to support this conclusion can be inferred from the ratio between  $\langle T_B \rangle$  and the blocking temperature determined from the Mössbauer spectra,  $T_{BM}$ . For a system of non-interacting particles the ratio  $T_{BM}/\langle T_B \rangle$  should be in the range 4–7 (Hanson et al. 1995), while for strongly interacting particles the ratio should be close to 1 (Morup et al. 1995). Since the human ferritin  $T_{BM}$  values lie in the range 30–38 K (Mann et al. 1987, St. Pierre et al. 1991), the ratio for the present case is equal to 4.5–5.6 for the liver and to 3.6–4.3 for the brain.

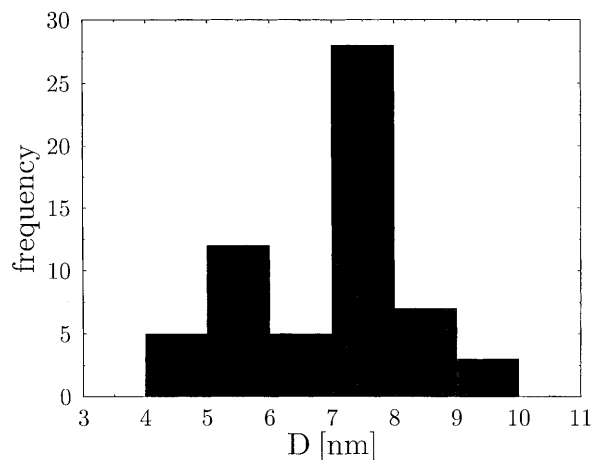


**Fig. 3** Size distribution of ferritin cores isolated from liver tissue

From the present magnetization curves one can also determine the irreversibility line. For this purpose the bifurcation temperature,  $T_B$ , has been plotted versus  $B$  in Fig. 7 for the liver and in Fig. 8 for the brain. In both cases,  $T_B$  decreases with  $B$ . For an ensemble of superparamagnetic particles, which should describe the ferritin-like cores, the behaviour can be theoretically described by the following formula (Mohie-Eldin et al. 1994):

$$B = a - bT_B^{1/2} \quad (2)$$

where  $a$  and  $b$  are constants and  $T_B$  is the blocking temperature.

The data shown in Figs. 7 and 8 were fitted with Eq. (2), and the best fits are marked by solid lines. The  $T_B$  values obtained are 18.8 K for the liver and 22.4 K for the brain. As can be seen, the quality of the fits with this ansatz was not very good ( $r^2 = 94.6\%$  for the liver and  $91.0\%$  for the brain). In particular, the curvature of the experimental points is obviously larger than that predicted by Eq. (2). In view of this, the data were also fitted with the formula normally used to describe the irreversibility line for spin-glasses:

$$B = c[1 - T_B/T_0]^{\phi/2} \quad (3)$$

where  $c$  is a constant and  $T_0$  is  $T_B$  at  $B = 0$ . For  $\phi = 3$  the irreversibility line is known as the AT line (de Almeida and Thouless 1978) and for  $\phi = 1$  it is called the GT line (Gay and Toulouse 1981). The use of Eq. (3) to describe our data seems also to be justified by the fact that for both classes of materials, i.e. superparamagnetic and spin-glass

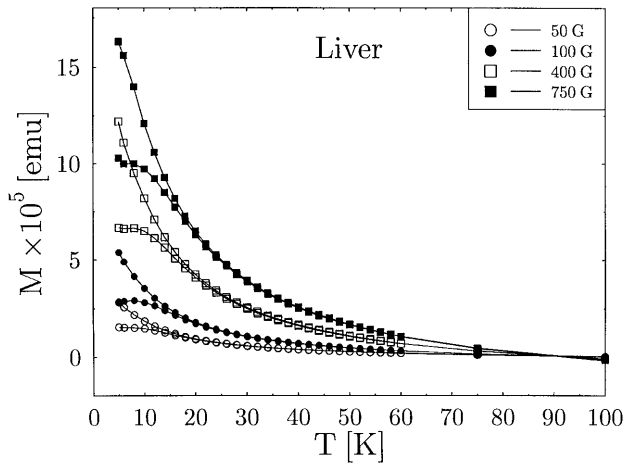


**Fig. 4** Examples of magnetization curves recorded with a SQUID magnetometer for the liver sample in various external magnetic fields

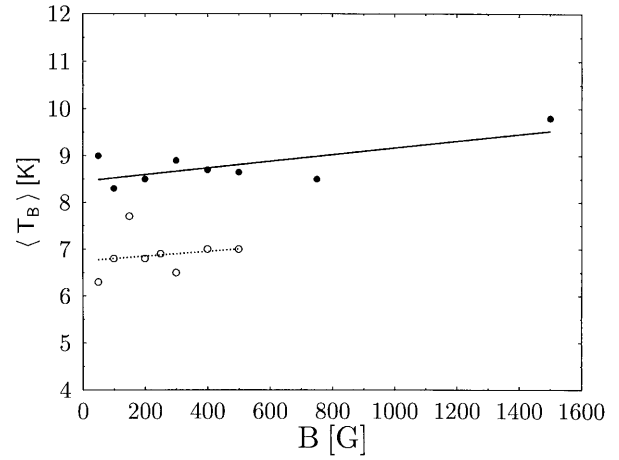


**Fig. 6** The average blocking temperature,  $\langle T_B \rangle$ , versus the external magnetic field,  $B$ , for the liver (open symbols) and the brain (full symbols). The straight lines show the best fits to the data

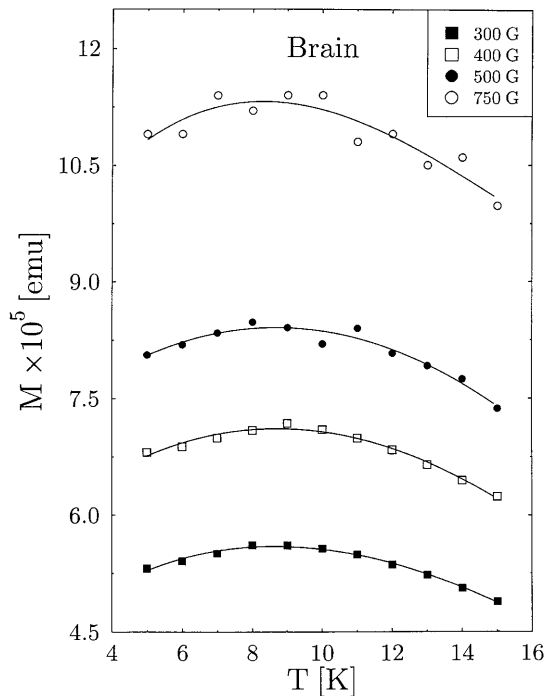


**Fig. 5** Examples of the maxima in the  $M_{ZFC}$  vs.  $T$  curves for the brain sample. The curves show the best fits to the data

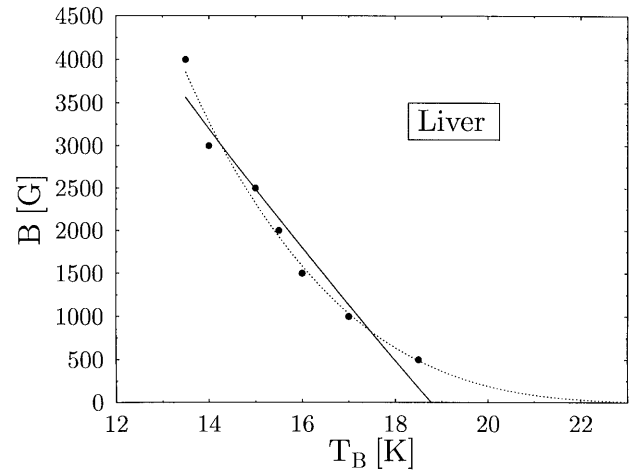


**Fig. 7** The irreversibility line in the  $B$ - $T$  plane for the liver. The solid line represents the best fit to the data with Eq. (2), while the dotted line is with Eq. (3)

ones, the magnetization curves  $M_{ZFC}$  versus  $T$  and  $M_{FC}$  versus  $T$  are virtually identical (see, for comparison, Chamberlin et al. 1982). Fitting the present data with Eq. (3) resulted in significantly better fits: see the dotted lines in Figs. 7 and 8 ( $r^2 = 98.3\%$  for the liver and  $99.6\%$  for the brain). The zero-field  $T_B$  values obtained in this way are equal to 25.1 K for the liver and 39.2 K for the brain. The  $\phi$  values are 7.3 for the liver and 11.7 for the brain. It should be noted that in real spin-glasses the exponent  $\phi$  is usually larger than 3 (Zieba and Lodziana 1996). It is equal to 7 at the ferro-para-spin-glass multicritical point, where the ferromagnetic interactions set in (Toulouse 1980). The value

of  $\phi$  obtained in the present case suggests that the ferritin-bound iron atoms behave in an external magnetic field rather like ferromagnetic spin-glasses and not like superparamagnetic particles (the average magnetic moment per core was estimated as  $\approx 100 \mu_B$  (Mohie-Eldin et al. 1994)). The dependence of  $T_B$  on  $B$  suggests that there is a spatial disorder of the magnetic moments similar to that found in spin-glasses.

Finally, based on the  $T_B$  values obtained from the SQUID data and the average core diameters obtained from the TEM measurements, the uniaxial magnetic anisotropy constant,  $K$ , was determined using the approximation

$$KV = k_B T_B \quad (4)$$

assuming spherically shaped particles. The values obtained for  $K$  are  $6 \times 10^3 \text{ J/m}^3$  for the liver sample and  $4 \times 10^4 \text{ J/m}^3$  for the brain sample.

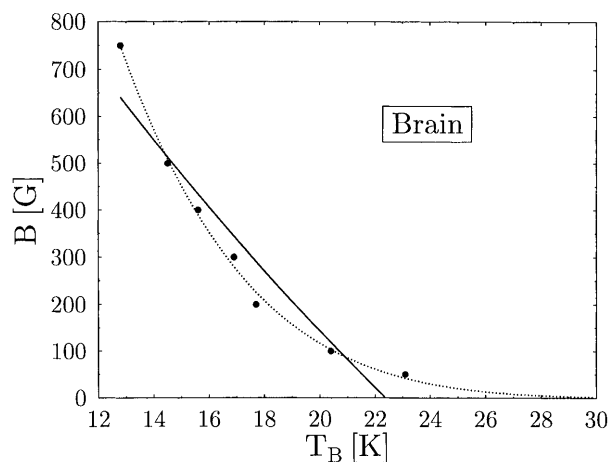


**Fig. 8** The irreversibility line in the  $B$ - $T$  plane for the brain. The solid line represents the best fit to the data with Eq. (2), while the dotted line is with Eq. (3)

The enhancement of  $K$  for smaller particles agrees with other data (Hanson et al. 1995), and it can be ascribed to a larger contribution to the total anisotropy from the surface in the case of the smaller brain-ferritin cores. It is worth noting that the value of  $K$  obtained presently for the brain agrees well with that found for amorphous  $\text{Fe}_{1-x}\text{C}_x$  particles having a similar size (Hanson et al. 1995).

## Conclusions

Based on the results presented in this study, the following conclusions can be drawn:

1. The concentration of iron present in the human brain (*globus pallidus*) amounts to 1.5(3) mg and that in the liver to 2.4(5) mg per gram of lyophilized tissue.
2. About 61–88% of the iron present is in the ferritin-like form, the rest being a low-spin iron.
3. Ferritin cores found in the liver are one order of magnitude larger than those in the brain.
4. The average blocking temperature was determined to be equal to 6.7 K for the liver and 8.5 K for the brain.
5. The maximum blocking temperature was 25.1 K for the liver and 39.2 K for the brain.

6. Investigated ferritin-like cores behave like non-interacting particles.
7. The irreversibility line can be better described in terms of a spin-glass formula with the  $\phi$  exponent characteristic of ferromagnetic interactions between the spins.
8. The uniaxial magnetic anisotropy constant was determined as  $6 \times 10^3 \text{ J/m}^3$  for the liver and  $4 \times 10^4 \text{ J/m}^3$  for the brain.

**Acknowledgements** J. Galazka-Friedman and A. Friedman are acknowledged for the kind supply of the samples. In addition, one of us (S. M. D.) wishes to thank the State Research Committee (KBN), Warsaw, for financial support.

## References

- Almeida RL de, Thouless DJ (1978) Stability of the Sherrington-Kirkpatrick solution of a spin glass model. *J Phys A* 11:983–990
- Bauminger ER, Nowik I (1998) Iron in Parkinson disease, blood diseases, malaria and ferritin. *Hyperfine Interact* 111:159–170
- Gabay M, Toulouse G (1981) Coexistence of spin-glass and ferromagnetic orderings. *Phys Rev Lett* 47: 201
- Galazka-Friedman J, Friedman A (1997) Controversies about iron in Parkinsonian and control substantia nigra. *Acta Neurobiol* 57: 217–225
- Hanson M, Johansson C, Morup S (1995) The influence of particle size and interactions on the magnetization and susceptibility of nanometer-size particles. *J Phys Condens Matter* 7:9263–9277
- Lauffer RB (1992) Iron in human disease. CRC Press, Boca Raton
- Luo W, Nagel SR, Rosenbaum TF, Rosenzweig RE (1991) Dipole interactions with random anisotropy in a frozen ferrofluid. *Phys Rev Lett* 67:2721–2724
- Mann S, Williams JM, Treffy A, Harrison PM (1987) Reconstituted and native iron-cores of bacterioferritin and ferritin. *J Mol Biol* 198: 405–416
- Mohie-Eldin M-EY, Frankel RB, Gunther L (1994) A comparison of the magnetic properties of polysaccharide iron complex (PIC) and ferritin: *J Magn Magn Mater* 135:65–81
- Morup S, Bodker F, Hendriksen PV, Linderroth S (1995) Spin-glass-like ordering of the magnetic moments of interacting nanosized maghemite particles. *Phys Rev B* 52:287–294
- Pierre TG St, Tran KC, Webb J, Macey DJ, Pootrakul P (1991) Mechanisms and phylogeny of mineralization in biological systems. Springer, Berlin Heidelberg New York pp 291–295
- Pierre TG St, Richardson DR, Baker E, Webb J (1992) A low-spin iron complex in human melanoma and rat hepatoma cells and a high-spin iron(II) complex in rat hepatoma cells. *Biochim Biophys Acta* 1135:154–158
- Toulouse G (1980) On the mean field theory of mixed spin glass-ferromagnetic phases. *J Phys (Paris) Lett* 41: L447–L449
- Zieba A, Lodziana Z (1996) Effective exponents for de Almeida-Thouless line. *Phase Trans* 57:161–171